HHS Public Access

Author manuscript

J Mech Behav Biomed Mater. Author manuscript; available in PMC 2019 January 01.

Published in final edited form as:

J Mech Behav Biomed Mater. 2018 January ; 77: 557–565. doi:10.1016/j.jmbbm.2017.10.001.

Durability of Adhesive Bonds to Tooth Structure Involving the DEJ

Enas Elbahie[1], **Dylan Beitzel**[1], **Mustafa Murat Mutluay**[1,2], **Hessam Majd**[1], **Mobin Yahyazadehfar**[1], and **Dwayne Arola**[3,4,5,♠]

[1]Department of Mechanical Engineering, University of Maryland Baltimore County, Baltimore, MD, USA [2]Adhesive Dentistry Research Group, Department of Cariology, Institute of Dentistry, University of Turku, Turku, Finland [3]Department of Materials Science and Engineering, University of Washington, Seattle, WA USA [4]Department of Restorative Dentistry, School of Dentistry, University of Washington, Seattle, WA USA [5]Department of Oral Health, School of Dentistry, University of Washington, Seattle, WA USA

Abstract

The importance of the Dentin Enamel Junction (DEJ) to the durability of adhesive bonds to tooth structure is unclear. In fact, no investigation has been reported on contributions of the DEJ to the fatigue resistance of the bonded interface. In this study, the durability of adhesive bonds to tooth structure involving the DEJ was quantified and compared to that of adhesive bonds to enamel only, not including the DEJ. Two different configurations of enamel bonding were considered, including when tensile stress is focused on the outer enamel (occlusal configuration) or the inner decussated enamel (decussated configuration). The resistance to failure for all bonded interfaces was assessed under both static and cyclic loading to failure. Results showed that the durability of the bonded interfaces was primarily a function of their resistance to crack initiation and growth. The bonded interface strength involving the DEJ was significantly ($p \leq 0.05$) greater than that of bonds to enamel only with occlusal configuration, under both static and cyclic loading. While the fatigue strength of bonds involving the DEJ was approximately 20% greater than that for enamel bonds with occlusal configuration (7.7 MPa) it was lower than that of enamel with the decussated configuration. The DEJ deterred cracks from extending readily into the dentin but it did not prevent fatigue failure. These results suggest that the durability of bonds to enamel are most dependent on the enamel rod decussation and that the DEJ plays a minor role.

Keywords

Bonding; Dentin Enamel Junction (DEJ); Durability; Enamel; Fatigue; Fracture; Resin Composite

♠**Corresponding Author**: Dwayne D. Arola, Ph.D., Department of Materials Science and Engineering University of Washington, Roberts Hall, 333; Box 352120 Seattle, WA 98195-2120 USA, darola@uw.edu, (206) 685-8158 (v) (206) 543-3100 (f).

INTRODUCTION

In the field of restorative dentistry, tooth structure that is undermined by caries is removed using dental burs and replaced with a restorative material of appropriate color and mechanical properties (Fig. 1). In today's practice, resin composites are the most common restorative material. These materials are light-curing particulate reinforced monomers. They are bonded to tooth structure, including the dentin and enamel, using resin adhesives.

One of the primary contributions to the failure of adhesive bonds to tooth structure is degradation by cyclic loading and fatigue [Van Meerbeek et al., 2003; Spencer et al., 2010; Pashley et al., 2011]. Surprisingly though, the performance of adhesive bonds to dentin and enamel has been assessed primarily by microtensile tests and static loads to failure [Pashley et al., 1999; De Munck et al., 2005a]. The fatigue properties of the bonded interface, which define its resistance to failure under cyclic loading, has received rather limited attention overall. In addition, contraction stresses develop in the resin composite as a result of light curing and generate residual tensile stresses [Yamamoto et al., 2011]. These stresses can facilitate cracking and further decreases the fatigue resistance of the bonded interface between the restoration and tooth structure.

The durability of adhesive bonds to tooth structure is a major concern in the field of restorative dentistry and the majority of studies on this topic have focused on dentin bonding [Arola, 2017]. In comparison, relatively few studies have been focused on the fatigue properties of adhesive bonds to enamel [Ruse et al., 1995; De Munck et al., 2005b; Erickson et al., 2006; 2008; 2009a; Barkmeier et al., 2009]. In studies comparing the durability of adhesive bonds to dentin and enamel, the fatigue resistance of enamel bonds is substantially lower than that for dentin [De Munck et al., 2005b; Yahyazadehfar et al. 2013a]. For instance, Yahyazadehfar et al. [2013a] reported that the apparent endurance limit of the bonded interface to enamel was nearly 40% lower than that achieved in bonding to dentin. Surprisingly, fatigue failure occurred through the initiation and propagation of cracks in the enamel and not by failure of the adhesive. If that is the predominate mode of failure in bonds involving enamel, using restorative approaches that are capable of arresting the damage and preventing crack propagation from the enamel to the underlying dentin could have clinical impact.

Cracks that initiate in the enamel on the occlusal surface of teeth must pass through the Dentin Enamel Junction (DEJ) to reach the underlying dentin and pulp. The DEJ is a complex interface that has been considered one of the most interesting in nature [Marshall et al., 2001; Marshall et al., 2003]. The width of this interface is under debate, with measures of just over a few microns [Habelitz et al., 2001] to an average of 10 μm and more [Gallagher et al., 2003; Fong et al., 1999]. Studies focused on the region surrounding the DEJ using nanoindentation have shown that the elastic modulus and hardness undergo a gradual transition from the hard and stiff qualities of the enamel to those of the more compliant and soft dentin [Fong et al., 1999; Marshall et al., 2001]. Perhaps the most interesting quality of the DEJ is its apparent contribution to the resisting crack extension from the enamel towards the dentin [Lin and Douglas, 1994; Xu et al., 1998; Marshall et al., 2003; Imbeni et al., 2005]. Prior evaluations concerned with the fracture resistance of the

DEJ were not performed on restored tooth structure. Furthermore, although the mechanics of fracture at the adhesive interface between tooth structure and resin composite has been examined, no study has identified how the DEJ participates in resisting the growth of cracks within or near the bonded interface in restored teeth.

The studies concerning fracture of the DEJ suggest that its complex microstructure results in a number of unique toughening mechanisms that operate in concert to promote crack arrest [White et al., 2005]. Attempts at characterizing the fracture toughness of the DEJ have resulted in values ranging from roughly 0.5 MPa•$m^{0.5}$ to over 3 MPa•$m^{0.5}$ [Lin and Douglas, 1994; Marshall et al., 1997; White et al., 2000; Dong and Ruse, 2003; Imbeni et al., 2005]. These values are not substantially greater than those reported for dental enamel [Bajaj et al., 2009a; Bechtle et al., 2010; Yahyazadehfar et al., 2013b]. Therefore, it is not clear whether the DEJ or the enamel plays a more important role on the bonded interface durability of teeth restored with resin composite restorations.

The DEJ appears to bestow the tooth with resistance to fracture from cracks initiating within the enamel. It could serve an equally important role in resisting fatigue failure of resin composite restorations bonded to enamel. However, to the authors' knowledge, no study has evaluated the contributions of the DEJ to the durability of resin-enamel adhesive bonds under cyclic loading. In this investigation, a combination of efforts involving experiments and a finite element analysis were performed to determine if: 1) if the DEJ increases the durability of adhesive bonds to dental enamel, and 2) the DEJ is capable of arresting fatigue damage that develop in the enamel of restored teeth. The overall objective was to develop new understanding concerning the contribution of the DEJ to the durability of adhesive bonds to tooth structure.

MATERIALS AND METHODS

Twin Bonded Interface (TBI) specimens were prepared from sections of caries-free human third molars that were obtained from participating clinics in the state of Maryland. The teeth were obtained with record of donor age (18≤age≤30) and gender according to a protocol approved by the University of Maryland Baltimore County (#Y04DA23151). The teeth were stored in Hank's Balanced Salt Solution (HBSS) for less than 1 month, and then sectioned using a slicer/grinder (Chevalier Smart-H818II, Chevalier Machinery, Santa Fe Springs, CA, USA) with diamond abrasive slicing wheels (#320 mesh abrasives) and copious water spray. Sections of enamel, or dentin and enamel encompassing the DEJ, were obtained from the cuspal regions of the donor teeth as shown in Figure 2(a).

The specimens were prepared using a special molding technique after Mutluay et al. [2013a, 2013b] and Yahyazadehfar et al., [2013a]. Briefly, the lingual and buccal aspects of the enamel cubes were etched for 15 sec (34% phosphoric acid gel), followed by application of primer to these surfaces according to the manufacturer's instructions. Adhesive was applied to the primed surfaces (Clearfil SE Bond, Lot 062127, Kuraray America) and cured for 10 sec with a quartz-tungsten-halogen light-curing unit (Demetron VCL 401, Demetron) with calibrated output intensity of 600 mW/cm^2 and tip diameter wider than 10 mm. The cubes were then placed centrally in a mold and resin composite (Clearfil AP-X, A2 color, Lot

1136AA; Kuraray America) was applied incrementally to the sides with adhesive to obtain beams with cross section of 2×2 mm^2 and 12 mm length. The composite was light-cured for 30 seconds on each side. The molded sections were released from the mold, polished to obtain smooth surfaces and then stored in HBSS at room temperature (22° C) for at least 24 hours. For quasi-static loading evaluations, ten specimens of three different groups were prepared, including occlusal enamel (control), decussated enamel and the DEJ, for a total of 30 specimens. For the cyclic loading evaluation, a total of 30 DEJ bonded interface specimens were prepared and tested. For the enamel, 30 specimens were evaluated with decussated orientation and 45 specimens were evaluated with occlusal orientation, which served as the control. Thirty of the occlusal enamel specimens were also part of an earlier study concerning the durability of enamel bonds [Yahyazadehfar et al. 2013a] and 15 additional tests were conducted to achieve the total 45. Therefore, the results presented include 30 + 30 + 45 = 105 specimens total.

Quasi-static and cyclic four-point flexure (Fig. 2(b)) was performed at room temperature with specimens in HBSS bath using a universal testing system (EnduraTEC Model ELF 3200, BOSE) with load capacity and sensitivity of 225 N and ±0.01 N, respectively. As previously indicated, the enamel specimens were evaluated using two different configurations. In the “occlusal” configuration, the outer enamel was placed on the tensile side of the flexure loading arrangement. That configuration is most consistent with the clinical condition where the tooth’s occlusal surface is subjected to the largest magnitude of tensile stress. Similarly, a “decussated” configuration was also examined with the inner enamel placed on the tensile side of the flexure loading arrangement. In that configuration, the decussated enamel is subjected to the maximum cyclic tensile stress. Assuming that cyclic loading induces damage on the tensile side of the beams, a comparison of the two different enamel orientations enables an assessment of the importance of decussation to crack initiation and growth resistance. For the interested reader, a description of enamel decussation is available in [Macho et al., 2003; Jiang et al., 2003]. For the DEJ specimens, the enamel side was always placed on the tensile side of the flexure arrangement and the DEJ was approximately at the central region of the specimen thickness as shown in Figure 2(b). In this last configuration, damage that develops in the enamel must pass across the DEJ to enable fracture of the bonded interface. The value of using the TBI specimen is that one of the interfaces undergoes fracture and enables a determination of the fatigue life. The second “twin” interface was subjected to the same cyclic loading and can be used to examine damage that results from the cyclic loading process.

Quasi-static loading to failure was performed under displacement control at a rate of 0.06 mm/min. The flexural strength (S) of the beams was estimated using conventional beam theory [Popov, 1978] in terms of the maximum measured load (P) and beam geometry (width b, thickness h) according to $S=3Pl/bh^2$, where l is the distance from interior and exterior supports (l=3 mm). The flexure strengths were compared using a one-way ANOVA and Tukey’s HSD post-hoc analysis with the critical value (alpha) set at 0.05.

Cyclic loading of all the specimens was conducted using the same four-point configuration (Fig. 2(b)) under load control with frequency of 4 Hz and stress ratio (R = ratio of minimum to maximum cyclic load) of 0.1. Fatigue testing was initiated using a maximum cyclic stress

of approximately 90% of the flexural strength identified from the quasi-static experiments. For successive specimens, the maximum cyclic load was decreased in increments of 1 MPa or less according to the staircase method of evaluation [Collins, 1981]. The process continued until reaching a cyclic stress amplitude at which the specimens did not fail within 1.2×10^6 cycles. Fatigue life diagrams were constructed from the stress amplitude and number of cycles to failure data for each group, and the results were fit using non-linear regression with a Basquin-type model [Stephens et al., 2001] according to

$$\sigma = \mathrm{A}(\mathrm{N})^{\mathrm{B}} \quad (1)$$

where A and B are the fatigue-life coefficient and exponent, respectively. The constants were obtained from a power law regression of the fatigue responses. The apparent endurance limit was estimated using the models for a fatigue limit defined at 1×10^7 cycles, which is consistent with previous studies of the bonded interface [Mutluay et al., 2013a; 2013b; Yahyazadehfar et al., 2013a]. The fatigue life distributions were compared using the Wilcoxon Rank-Sum Test with $p \leq 0.05$ considered significant.

Selected specimens were evaluated by Scanning Electron Microscopy (SEM) with a JEOL Model JSM-5600 using either secondary electron imaging (SEI) or back scattered electron (BEC) imaging mode. Prior to this analysis, the specimens were dehydrated in an ascending ethanol series (70–100%), fixed in Hexamethyldisilazane, polished lightly in series using #800, #2400 and #4000 emory cloth and then sputtered with gold/palladium to enhance conductance of the hard tissue and resin adhesive. The fracture surfaces were inspected to identify the origins of failure and potential contributing mechanisms to degradation under cyclic loading.

Numerical Model and Analysis

The flexure specimen geometry adopted for evaluating the resin-enamel bond strength was designed with two identical interfaces, after the double-notched beam commonly used for evaluating engineering and natural materials [e.g. Nalla et al., 2003]. Both interfaces are subjected to a constant bending moment and a corresponding equivalent normal stress. One of the twin interfaces undergoes failure and the second interface effectively “freezes” the status of the microstructure at that moment, thereby providing an interface for evaluation that has undergone cycle loading, but has not fractured. Due to the unique geometry, it was necessary to evaluate the stress distribution resulting from flexural loading of the resin-DEJ specimens using a finite element model. An equivalent evaluation of the stress distribution within the resin- enamel specimens was conducted using finite element analysis and previously reported [Mutluay et al., 2013a; Yahyazadehfar et al., 2013a]. The purpose of this finite element analysis was simply to understand the stress distribution across the bonded interfaces involving either the enamel or the DEJ, and to use that knowledge in further understanding the interface failures of the TBI specimens resulting from static and cyclic loading.

A two-dimensional finite element analysis was performed using commercial software (ABAQUS 6.7-3; Dassault Systèmes Americas Corp., Waltham, MA, USA). A full model

was developed for the beam to simulate the resulting stress and strain distribution. The beam was subjected to simulated flexural loading according to the experimental configuration in Fig. 2(b), through rigid pins. The pins were defined as rigid body shells with frictionless contact between the pins and beam surfaces. The model beam was defined having four regions (Fig. 3(a)) including the resin composite, resin adhesive and enamel and dentin (as appropriate), and meshed with approximately 1200 type CPE4 plane strain elements. The materials were treated as linear elastic with elastic modulus (E) and Poisson's ratio (ν) defined for resin composite (6.0 GPa, 0.26) [AP-X, Kuraray USA], resin adhesive (4.4 GPa, 0.24) [Magni et al., 2010], enamel (E=35 GPa, ν=0.29) and dentin (E=15 GPa, ν=0.29) [Arola and Reprogel, 2006]. The elastic modulus assigned for enamel is based on a macroscopic scale characterization [Ang et al., 2010; Bechtle et al., 2010] and is smaller than that typically found using nanoindentation (roughly 70 to 100 GPa) [Park et al., 2008; Cuy et al., 2002].

Results of the finite element analysis for flexural loading of the bonded interface specimen included the normal strain (ε_x) and normal stress (σ_x) distributions within the region of constant bending moment, and are shown in Fig. 3(b) and Fig. 3(c), respectively. These distributions result from a flexure load of 10 Newtons, which is within the range of applied experimental loads. As evident in Fig. 3(b), there is a concentration in normal strain within the adhesive, which is greatest near the tensile and compressive surfaces. The largest strain develops within the resin adhesive, and is substantially larger than that within the adjacent materials (up to a factor of 7x). In addition, there is a stress concentration in the composite that develops at the point of contact loading, which is apparent in Fig. 3(c).

The maximum normal stress obtained from the model occurs on the tensile side of the flexure specimen and is plotted as a function of distance from the specimen's axis of symmetry in Fig. 4. To be consistent with the range of experimental conditions, results are shown for enamel bonding (Fig. 4(a)) and for bonding with the DEJ (Fig. 4(b)) as describe schematically in Fig. 3(a). For comparison, the normal stress predicted using beam theory for a homogeneous specimen with identical geometry and loading configuration is presented in this figure as well. It is important to highlight that although the interfaces are located within one millimeter of the two interior loading pins, the tensile stress distribution is not influenced substantially by the contact stresses. Nevertheless, the normal stress is not constant between the two central loading pins as a result of the adhesive interface. Note that for both bonding scenarios, there is a concentration of stress that develops in the enamel, adjacent to the bonded interface. The stress concentration is caused by the elastic modulus mismatch and is greatest for enamel bonding only, without the DEJ. Based on a comparison of the numerical results with beam theory, the largest stress develops in the enamel and is approximately 16% greater than that predicted using beam theory. For the DEJ specimens, the largest stress is approximately 10% greater than that predicted using beam theory. For consistency in definition, all of the stresses reported at failure in the experiments are those estimated using beam theory.

RESULTS

The average flexure strength of the specimens with adhesive bonds to the enamel and DEJ substrates is shown in Figure 5. The strength of the enamel bonds with occlusal orientation was 19.9±3.9 MPa. That value was significantly lower ($p \leq 0.05$) than the strength of enamel bonds in the decussated orientation (27.9 ± 6.5 MPa), but not for specimens including the DEJ (24.2±7.1 MPa). There was no significant difference ($p > 0.05$) between the flexure strengths of the adhesive bonds to enamel in the decussated orientation and the DEJ.

The results of the cyclic loading experiments are shown in Figure 6. A fatigue life diagram for results of the enamel specimens with occlusal orientation is shown in Figure 6(a). Note that the results in this figure span lives from 1 to over 1 million cycles and those data points with arrows represent specimens that did not fail within 1.2 million cycles. A fatigue life diagram comparing results for the enamel with occlusal and decussated orientations is shown in Figure 6(b). Note that the comparison is shown for all results of fatigue life ≥ 100 cycles. The fatigue life distributions are presented with power law models describing the mean fatigue strength over the range in lives evaluated. According to results of the Wilcoxon Rank-Sum test, the fatigue strength for the decussated orientation was significantly greater than that of the occlusal orientation ($Z = -6.32$; $p < 0.0001$).

A comparison of the fatigue responses of the DEJ bonded interface specimens and the enamel specimens with occlusal orientation is shown in Figure 6(c). As evident in this figure, the fatigue strength of the DEJ bonded interface specimens was significantly greater than that of the enamel control ($Z = -5.53$; $p < 0.0001$). Results of the power law model are also presented for the DEJ bonded specimens in Fig. 6(c). Surprisingly, the fatigue strength of the bonded interfaces to the decussated enamel was significantly greater than that for bonding to the DEJ ($Z = -2.26$; $p = 0.024$).

The power law models describing the mean fatigue strength distribution were used to estimate an “apparent” endurance limit at a fatigue limit of 1×10^7 cycles. Using that approach, the apparent endurance limit obtained for the enamel specimens with occlusal orientation (7.7 MPa) was the lowest of the three bonded interfaces examined. The values estimated for the enamel with decussated orientation (9.9 MPa) and the DEJ (9.6 MPa) were both approximately 20% greater than that of the control, but were not substantially different from one another.

Micrographs detailing characteristics of the fracture surfaces from selected enamel specimens are shown in Figure 7. Fracture initiated on the tensile surface under both quasi-static and cyclic loading for all bonding configurations that were evaluated. For those specimens with occlusal orientation, fatigue failure occurred within the enamel as shown from the fracture surface of an enamel specimen with occlusal orientation in Figure 7(a). A similar view of the fracture surface for an enamel specimen with decussated orientation is shown in Figure 7(b). For the majority of specimens evaluated, fracture initiated and progressed along the interface of adjacent enamel rods, regardless of the bonding configuration. Evidence that failure initiated and progressed in enamel is most clearly seen in the features of a specimen with decussated enamel orientation in Figure 7(c). This view is

from the surface of maximum tensile stress and highlights the composite (C), resin adhesive (A) and enamel (E). The crack in this specimen is within 5 μm of the enamel/adhesive interface and extends adjacent and parallel to the adhesive of the bonded interface. In addition, individual enamel rods are highlighted in this figure (arrows). The protein-rich portion of the interrod enamel appears to have been partially separated as a result of the cyclic tensile stress, which is evident from the faint view of the oval enamel rods on the surface.

Fracture of the bonded interface specimens involving the DEJ most frequently initiated within the enamel. Consistent with the specimens involving adhesive bonds to enamel only, failure generally initiated within a few micrometers from the bonded interface as shown in Figure 8(a). The interface in this figure is the twin interface that did not failure, but exhibits the damage associated with cyclic loading. The crack opening gap is approximately 5 μm in width, which is substantially greater than for the enamel bonded specimens. An example of the path of crack extension in enamel from the tensile surface to the DEJ bonded specimen is shown in Figure 8(b); this is a side view of the specimen with the maximum tensile surface in the horizontal plane and located above the field of view in the image. The crack follows the interface of the enamel rods, which are not straight, as evident for the fracture surface in Figure 8(b). For those specimens where initiation occurred in the enamel, the crack progressed within the decussated enamel until reaching the DEJ, as evident in this figure, and the more highly magnified view in Figure 8(c). The crack appears temporarily arrested at the DEJ. Small cracks are also evident that extend from the DEJ into the enamel. This is a common observation for the specimens in this group, and appears to occur from cracks that initiate from the enamel tufts as commented by Myoung et al., [2009].

DISCUSSION

The present study evaluated the importance of the DEJ to the durability of adhesive bonds to tooth structure for the first time. Results of the experiments showed that bonds to enamel that involved the DEJ were significantly more durable than those without it, provided that failure initiated from the tooth's exterior (occlusal enamel) and continued towards the DEJ. Nevertheless, the bonded interface specimens involving the DEJ did not provide the greatest durability of all the configurations evaluated in this investigation.

In relation to the number of studies on the strength of dentin and enamel bonds, few studies have involved bonding to the DEJ or considered its importance. Shimada et al. [2003] compared the shear bond strength achieved using Clearafil SE Bond with substrates of dentin, enamel and the DEJ. No significant difference in shear strength was identified amongst the three substrates. However, in an investigation involving four different adhesives, Li et al. [2011] found that the greatest shear bond strength was achieved by dentin bonds, followed by the DEJ and then enamel. Mutluay et al. [2013a] evaluated dentin bonds with Clearafil SE in flexure using the twin bonded interface approach and reported an average strength of roughly 66 MPa. The rank in strength obtained in flexure (strength of dentin bonds≥ DEJ≥ enamel) from the present evaluation with Clearfil SE agrees with that of Li et al. [2011] for shear loading. While there is far less difference between the apparent endurance limits of the three substrates, they exhibit the same rank, with that obtained for

dentin (13 MPa from Mutluay et al. [2013a]) > DEJ (9.6 MPa) > enamel (7.7 MPa). If the response for the decussated enamel is considered (i.e. replacing the occlusal enamel), the rank of the DEJ and the enamel are exchanged. That could be considered of limited clinical relevance as it occurs when the largest tensile stress develops in deep decussated enamel rather than at the occlusal surface. Mastication generally causes the largest tensile stresses for typical Class I and Class III bonds at the cavosurface margins [Arola et al., 2001]. However, simulations of shrinkage stress in composites show stress concentrations develop at the DEJ [Kowalczyk, 2009] and the margins [Chuang et al., 2011; Boaro et al., 2014]. Thus, the larger fatigue strength of the adhesive bonds involving the DEJ does have clinical relevance.

Spatial variations in adhesive bond strength to dentin are not uncommon [Shimada and Tagami, 2003] and can be adhesive dependent [e.g. Toledano et al., 2003; Erickson et al., 2009b] as well as a function of the methods of application [Ando et al., 2008; Torres et al., 2009]. But the difference in durability between the enamel bonds with occlusal and decussated orientation is not attributed to simply the difference in enamel structure with location. In the occlusal orientation of enamel bonds the tensile region of the enamel exhibited prisms parallel to one another, without decussation, as evident in Figure 7(a). In these specimens, fracture initiated along the interface of adjacent rods. Closer to the neutral axis and within the compressive region the enamel microstructure transitioned into a decussated pattern of interwoven parazone and diazone regions. This is evident in the tensile aspect of the enamel bonds with decussated orientation, as shown in Fig. 7(b). The threshold stress intensity and initiation toughness of the inner decussated enamel are greater than that of the outer enamel [Bajaj and Arola, 2009b], which deters the growth of cracks from defects at the tensile surface. In addition, that combination of properties acts to suppress the initiation of fracture within the enamel in the decussated orientation of enamel bonds, and diverts failures to the next weakest link (e.g. resin adhesive and composite). Indeed, some of the enamel bonds failed due to initiation of cracks within the adhesive or within the composites in the decussated orientation, but this was uncommon. Evidently these adhesive bond failures occurred due to bonding defects. The superior durability of the decussated orientation of enamel bonding is believed to result from the larger fracture toughness of the decussated enamel and its contribution to resisting the growth of damage from the tensile surface.

Under both static and cyclic loading conditions, failure of the enamel bonds with occlusal orientation did not initiate within the adhesive bond but developed within the enamel rods adjacent to the interface. The occurrence of failure within the enamel and not the adhesive interface is a product of the stress distribution adjacent to the bonded interface. The tensile stress acting near the interface is largest in the enamel (Fig. 4(b)), and is due to a stress concentration that develops from the elastic modulus mismatch and higher modulus of enamel [Ausiello et al., 2002; Asmussen et al., 2008]. It is important to note that previous evaluations of the resin- enamel interface reported fatigue failure occurred in the adhesive or bonded interface, not in enamel [De Munck et al., 2005; Erickson et al., 2006; 2008; 2009a; Barkmeier et al., 2009]. That could be a consequence of the enamel rod orientation or as a result of the resin adhesive. These previous studies involved bonding to labial surfaces, and/or applied shear loading to the bonded interface where the resulting tensile stresses

oriented transverse to the axis of the rods was very low. The other plausible contribution is the difference in bond strength relative to Clearafil SE. Adhesives with lower strength would be more apt to fail in the adhesive.

Results of the finite element analysis (Fig. 4) show that the lower elastic modulus of the adhesive causes a stress concentration in the enamel, adjacent to the interface. As such, it could be conceived that failures using the twin bonded interface approach are predisposed to occur within the enamel. However, due to the compliance of the adhesive, that is also a characteristic of the stress distribution across the adhesive interface in restored teeth as well. Differences between the challenges of the oral environment and methods used for conducting in vitro evaluations have been under greater scrutiny [Kelly et al., 2012; Roulet, 2012; Söderholm, 2012]. Hence, the non-uniform stress distribution of the twin bonded interface approach may be considered one of its attractive qualities rather than a weakness.

Although the DEJ deterred crack extension from the enamel to dentin, as has been observed previously [e.g. Dong and Ruse, 2003, Imbeni et al., 2005] it did not completely arrest many of the cracks that reached it. After the cracks reached the DEJ they continued transversely along the DEJ until arriving at the bonded interface (not shown), at which bulk failure ensued. The DEJ was most effective at arresting cracks when the course of the enamel rods extended away from the bonded interface, as evident in Fig. 8(b).

There was a small, but significant difference between the fatigue strength distribution for specimens of enamel with decussated orientation and those involving the DEJ. This observation suggests that the decussated structure of the enamel rods is actually more effective than the DEJ at deterring the growth of cracks in enamel. Of course, the DEJ can serve to amplify the bonded interface durability when the damage extends from the enamel and towards the dentin. However, a large portion of the crack growth resistance that is interpreted to result from the DEJ actually comes from the decussated enamel rods and the toughening mechanisms that operate on the crack before it reaches the DEJ. In fact, the decussated enamel and the DEJ should be considered as partners that work together to prevent crack extension into the underlying dentin.

The findings of this investigation make a novel contribution to the literature, but there are recognized limitations to the evaluation that should be considered. Perhaps the primary limitation is that the experimental evaluation involves the use of only one resin adhesive and resin composite. Failure of the bonded interface, the contributing mechanisms and its durability is undoubtedly dependent on the restorative system. Less durable adhesive systems may result in fatigue failures more prominently at the resin-enamel interface, which would reduce the importance and dependence on the decussated enamel or the DEJ. The finite element model was used to understand the stress distribution in the specimen near the bonded interface to complement the fractographic evaluation of the fracture surfaces. The materials in the model were treated as a continuum, without detailed descriptions of the microstructure, and crack growth was not simulated. The finite element model could be used to perform a parametric study concerning the bonded joint and materials involved. That topic is worthy of a separate evaluation.

Another limitation to the investigation is that polymerization shrinkage stresses were not present across the bonded interface due to the specimen design and fabrication process. That is an important concern since shrinkage would cause the development of tensile stresses, which would increase the cyclic stress ratio (R=min stress/max stress). Fatigue strength generally decreases with an increase in stress ratio [Stephens et al., 2001]. As such, tensile residual stresses resulting shrinkage stresses would be expected to cause more rapid degradation and further reduction in durability of the interface. An increase in stress ratio could also promote more extensive creep deformation in the adhesive and hybrid layer, thereby promoting a change in the failure mechanisms. This issue is worthwhile to consider in future studies. Another limitation worth considering is that the testing environment did not include other forms of bonded interface attack, including biofilm exposure [Mutluay et al., 2013a], and the action of MMPs [Zhang et al., 2017]. These factors could be important to the relative merits of the DEJ, but were not considered. Despite the aforementioned concerns, the results further our understanding on the importance of the DEJ to adhesive bonds to tooth structure. They also serve as an important contribution to the growing base of knowledge concerning the degradation of adhesive bonds to tooth structure as a result of cyclic loading conditions.

CONCLUSION

An experimental evaluation of the strength and durability of resin-enamel and resin-DEJ bonded interfaces was conducted under monotonic and cyclic loading to failure. The initiation of bond failure occurred in tension in all specimens, and for most specimens occurred at the interface of the enamel prisms and not within the resin adhesive. Under monotonic loading the bonded interfaces involving the DEJ were 20% stronger than that not involving the DEJ for cracks extending from occlusal enamel. Similarly, the fatigue strength of bonded interfaces involving the DEJ was approximately 20% greater than that achieved by the enamel interface alone. Results showed the cyclic crack extension within the enamel is a viable mode of bonded interface failure involving composite restorations. The DEJ serves as an effective crack barrier, capable of diverting cracks within enamel from extending into the dentin. The effectiveness of the DEJ depends on the rod orientation, and is greatest when the rods extend away from the bonded interface. The enamel bonds were least durable when the outer enamel was subjected to cyclic tension, which is most likely to develop from shallow restorations and those that are subject to substantial resin composite shrinkage.

Acknowledgments

This study was supported in part by a seed grant from the University of Maryland Baltimore County (D. Arola) and an award from the National Institutes of Health (NIDCR R01 DE016904; Arola). The authors also gratefully acknowledge Kuraray America for their generous donation of bonding supplies and resin composite, and Prof. Frederick Rueggeberg of the Georgia Health Sciences University for kindly supplying and calibrating the light curing unit.

Support for the following investigation was provided in part by the National Institutes of Dental and Craniofacial Research (DE016904).

References

Ando S, Watanabe T, Tsubota K, Yoshida T, Irokawa A, Takamizawa T, Kurokawa H, Miyazaki M. Effect of adhesive application methods on bond strength to bovine enamel. J Oral Sci. 2008; 50(2): 181–6. [PubMed: 18587208]

Ang SF, Bortel EL, Swain MV, Klocke A, Schneider GA. Size-dependent elastic/inelastic behavior of enamel over millimeter and nanometer length scales. Biomaterials. 2010; 31(7):1955–63. [PubMed: 19969342]

Arola D, Galles LA, Sarubin MF. A comparison of the mechanical behavior of posterior teeth with amalgam and composite MOD restorations. J Dent. 2001; 29(1):63–73. [PubMed: 11137640]

Arola DD, Reprogel RK. Tubule orientation and the fatigue strength of human dentin. Biomaterials. 2006; 27(9):2131–40. [PubMed: 16253323]

Arola D. Fatigue testing of biomaterials and their interfaces. Dent Mater. 2017; 33(4):367–381. [PubMed: 28222907]

Asmussen E, Peutzfeldt A. Class I and Class II restorations of resin composite: an FE analysis of the influence of modulus of elasticity on stresses generated by occlusal loading. Dent Mater. 2008; 24(5):600–5. [PubMed: 17767951]

Ausiello P, Apicella A, Davidson CL. Effect of adhesive layer properties on stress distribution in composite restorations-a 3D finite element analysis. Dent Mater. 2002; 18(4):295–303. [PubMed: 11992906]

Bajaj D, Arola D. On the R-Curve behavior of human tooth enamel. Biomaterials. 2009a; 30(23–24): 4037–4046. [PubMed: 19427691]

Bajaj D, Arola D. Role of prism decussation on fatigue crack growth and fracture of human enamel. Acta Biomat. 2009b; 5(8):3045–3056.

Barkmeier WW, Erickson RL, Latta MA. Fatigue limits of enamel bonds with moist and dry techniques. Dent Mater. 2009; 25(12):1527–31. [PubMed: 19679342]

Bechtle S, Habelitz S, Klocke A, Fett T, Schneider GA. The fracture behaviour of dental enamel. Biomaterials. 2010; 31(2):375–84. [PubMed: 19793611]

Boaro LC, Brandt WC, Meira JB, Rodrigues FP, Palin WM, Braga RR. Experimental and FE displacement and polymerization stress of bonded restorations as a function of the C-Factor, volume and substrate stiffness. J Dent. 2014; 42(2):140–8. [PubMed: 24296164]

Chuang SF, Chang CH, Chen TY. Contraction behaviors of dental composite restorations--finite element investigation with DIC validation. J Mech Behav Biomed Mater. 2011; 4(8):2138–49. [PubMed: 22098914]

Collins, JA. Fatigue of Metals in Mechanical Design. John Wiley and Sons; 1981. Fatigue Testing Procedures and Statistical Interpretations of Data.

Cuy JL, Mann AB, Livi KJ, Teaford MF, Weihs TP. Nanoindentation mapping of the mechanical properties of human molar tooth enamel. Arch Oral Biol. 2002; 47(4):281–91. [PubMed: 11922871]

De Munck J, Van Landuyt K, Peumans M, Poitevin A, Lambrechts P, Braem M, Van Meerbeek B. A critical review of the durability of adhesion to tooth tissue: methods and results. J Dent Res. 2005a; 84(2):118–32. [PubMed: 15668328]

De Munck J, Braem M, Wevers M, Yoshida Y, Inoue S, Suzuki K, Lambrechts P, Van Meerbeek B. Micro-rotary fatigue of tooth-biomaterial interfaces. Biomaterials. 2005b; 26(10):1145–53. [PubMed: 15451634]

Dong XD, Ruse ND. Fatigue crack propagation path across the dentinoenamel junction complex in human teeth. J Biomed Mater Res A. 2003; 66(1):103–9. [PubMed: 12833436]

Erickson RL, De Gee AJ, Feilzer AJ. Fatigue testing of enamel bonds with self-etch and totaletch adhesive systems. Dent Mater. 2006; 22(11):981–7. [PubMed: 16364421]

Erickson RL, De Gee AJ, Feilzer AJ. Effect of pre-etching enamel on fatigue of self-etch adhesive bonds. Dent Mater. 2008; 24(1):117–23. [PubMed: 17482672]

Erickson RL, Barkmeier WW, Kimmes NS. Fatigue of enamel bonds with self-etch adhesives. Dent Mater. 2009a; 25(6):716–20. [PubMed: 19150125]

Erickson RL, Barkmeier WW, Latta MA. The role of etching in bonding to enamel: a comparison of self-etching and etch-and-rinse adhesive systems. Dent Mater. 2009b; 25(11):1459–67. [PubMed: 19665220]

Fong H, Sarikaya M, White SN, Snead ML. Nano-mechanical properties profiles across dentin–enamel junction of human incisor teeth. Mater Sci Engr. 1999; 7(2):119–128.

Gallagher RR, Demos SG, Balooch M, Marshall GW Jr, Marshall SJ. Optical spectroscopy and imaging of the dentin-enamel junction in human third molars. J Biomed Mater Res A. 2003; 64(2): 372–7. [PubMed: 12522825]

Habelitz S, Marshall SJ, Marshall GW Jr, Balooch M. The functional width of the dentinoenamel junction determined by AFM-based nanoscratching. J Struct Biol. 2001; 135(3):294–301. [PubMed: 11722169]

Imbeni V, Kruzic JJ, Marshall GW, Marshall SJ, Ritchie RO. The dentin–enamel junction and the fracture of human teeth. Nat Mater. 2005; 4:229–232. [PubMed: 15711554]

Jiang Y, Spears IR, Macho GA. An investigation into fractured surfaces of enamel of modern human teeth: a combined SEM and computer visualisation study. Arch Oral Biol. 2003 Jun; 48(6):449–57. [PubMed: 12749917]

Kelly JR, Benetti P, Rungruanganunt P, Bona AD. The slippery slope: critical perspectives on in vitro research methodologies. Dent Mater. 2012; 28(1):41–51. [PubMed: 22192250]

Kowalczyk P. Influence of the shape of the layers in photo-cured dental restorations on the shrinkage stress peaks-FEM study. Dent Mater. 2009; 25(12):e83–91. [PubMed: 19786300]

Kotousov A, Kahler B, Swain M. Analysis of interfacial fracture in dental restorations. Dent Mater. 2011; 27(11):1094–101. [PubMed: 21824651]

Li F, Liu X, Zhang L, Shen L, Chen J. Bonding efficiency of contemporary adhesives to the dentinoenamel junction zone. Eur J Oral Sci. 2011; 119(3):232–40. [PubMed: 21564318]

Lin CP, Douglas WH. Structure-property relations and crack resistance at the bovine dentinenamel junction. J Dent Res. 1994; 73(5):1072–1078. [PubMed: 8006234]

Macho GA, Jiang Y, Spears IR. Enamel microstructure--a truly three-dimensional structure. J Hum Evol. 2003 Jul; 45(1):81–90. [PubMed: 12890446]

Magni E, Ferrari M, Hickel R, Ilie N. Evaluation of the mechanical properties of dental adhesives and glass-ionomer cements. Clin Oral Investig. 2010; 14(1):79–87.

Marshall GW Jr, Balooch M, Gallagher RR, Gansky SA, Marshall SJ. Mechanical properties of the dentinoenamel junction: AFM studies of nanohardness, elastic modulus, and fracture. J Biomed Mater Res. 2001; 54:87–95. [PubMed: 11077406]

Marshall SJ, Balooch M, Habelitz S, Balooch G, Gallagher R, Marshall GW. The dentin-enamel junction- a natural, multilevel interface. J Eur Ceram Soc. 2003; 23:2897–2904.

Mutluay MM, Yahyazadefar M, Ryou H, Majd H, Arola D. Fatigue of the resin-dentin interface: A new approach for evaluating the durability of dentin bonds. Dent Mater. 2013a; 29(4):437–49. [PubMed: 23434232]

Mutluay MM, Ryou H, Zhang K, Yahyazadefar M, Majd H, Xu HHK, Arola D. On the durability of resin-dentin bonds after degradation by biofilm. J Mech Behav Biomed Mater. 2013b; 18:219–31. [PubMed: 23276517]

Myoung S, Lee J, Constantino P, Lucas P, Chai H, Lawn B. Morphology and fracture of enamel. J Biomech. 2009; 42(12):1947–51. [PubMed: 19559438]

Nalla RK, Kinney JH, Ritchie RO. On the fracture of human dentin: is it stress- or straincontrolled? J Biomed Mater Res. A. 2003; 67(2):484–95. [PubMed: 14566789]

Park S, Wang DH, Zhang D, Romberg E, Arola D. Mechanical properties of human enamel as a function of age and location in the tooth. J Mater Sci: Mater Med. 2008; 19(6):2317–24. [PubMed: 18157510]

Pashley DH, Carvalho RM, Sano H, Nakajima M, Yoshiyama M, Shono Y, Fernandes CA, Tay FR. The microtensile bond test: a review. J Adhes Dent. 1999; 1(4):299–309. [PubMed: 11725659]

Pashley DH, Tay FR, Breschi L, Tjäderhane L, Carvalho RM, Carrilho M, Tezvergil-Mutluay A. State of the art etch-and-rinse adhesives. Dent Mater. 2011; 27(1):1–16. [PubMed: 21112620]

Popov, EP. Mechanics of Materials. 2. Prentice Hall Inc; New Jersey: 1978.

Roulet JF. Is in vitro research in restorative dentistry useless? J Adhes Dent. 2012; 14(2):103–4. [PubMed: 22518387]

Ruse ND, Shew R, Feduik D. In vitro fatigue testing of a dental bonding system on enamel. J Biomed Mater Res. 1995; 29(3):411–5. [PubMed: 7615591]

Shimada Y, Iwamoto N, Kawashima M, Burrow MF, Tagami J. Shear bond strength of current adhesive systems to enamel, dentin and dentin-enamel junction region. Oper Dent. 2003; 28(5):585–90. [PubMed: 14531605]

Shimada Y, Tagami J. Effects of regional enamel and prism orientation on resin bonding. Oper Dent. 2003; 28(1):20–7. [PubMed: 12540114]

Söderholm KJ. Time to abandon traditional bond strength testing? J Adhes Dent. 2012; 14(1):3–4. [PubMed: 22518386]

Spencer P, Ye Q, Park J, Topp EM, Misra A, Marangos O, Wang Y, Bohaty BS, Singh V, Sene F, Eslick J, Camarda K, Katz JL. Adhesive/Dentin interface: the weak link in the composite restoration. Ann Biomed Eng. 2010; 38(6):1989–2003. [PubMed: 20195761]

Stephens, RI., Fatemi, A., Stephens, RR., Fuchs, HO. Metal Fatigue in Engineering. 2. John Wiley and Sons, Inc; New York: 2001.

Toledano M, Osorio R, Ceballos L, Fuentes MV, Fernandes CA, Tay FR, Carvalho RM. Microtensile bond strength of several adhesive systems to different dentin depths. Am J Dent. 2003; 16(5):292–8. [PubMed: 14677606]

Torres CR, Barcellos DC, Pucci CR, Lima GM, Rodrigues CM, Siviero M. Influence of methods of application of self-etching adhesive systems on adhesive bond strength to enamel. J Adhes Dent. 2009; 11(4):279–86. [PubMed: 19701508]

Van Meerbeek B, De Munck J, Yoshida Y, Inoue S, Vargas M, Vijay P, Van Landuyt K, Lambrechts P, Vanherle G. Buonocore memorial lecture. Adhesion to enamel and dentin: current status and future challenges. Oper Dent. 2003; 28(3):215–35. [PubMed: 12760693]

White SN, Paine ML, Wen Luo, Sarikaya M, Fong H, Zhaokun YU, Li ZC, Snead ML. The dentino-enamel junction is a broad transitional zone uniting dissimilar bioceramic composites. J Am Ceram Soc. 2000; 83:238–240.

White SN, Miklus VG, Chang PP, Caputo AA, Fong H, Sarikaya M, Luo W, Paine ML, Snead ML. Controlled failure mechanisms toughen the dentino-enamel junction zone. J Prosthet Dent. 2005; 94:330–335. [PubMed: 16198169]

Xu HH, Smith DT, Jahanmir S, Romberg E, Kelly JR, Thompson VP, Rekow ED. Indentation damage and mechanical properties of human enamel and dentin. J Dent Res. 1998; 77(3):472–80. [PubMed: 9496920]

Yahyazadehfar M, Mutluay MM, Majd H, Ryou H, Arola D. Fatigue of the resin-enamel bonded interface and the mechanisms of failure. J Mech Behav Biomed Mater. 2013a; 21:121–32. [PubMed: 23571321]

Yahyazadehfar M, Bajaj D, Arola DD. Hidden contributions of the enamel rods on the fracture resistance of human teeth. Acta Biomater. 2013b; 9(1):4806–14. [PubMed: 23022547]

Yamamoto T, Nishide A, Swain MV, Ferracane JL, Sakaguchi RL, Momoi Y. Contraction stresses in dental composites adjacent to and at the bonded interface as measured by crack analysis. Acta Biomater. 2011; 7(1):417–23. [PubMed: 20691287]

Zhang Z, Beitzel D, Mutluay M, Tezvergil-Mutluay A, Tay FR, Pashley DH, Arola D. Fatigue resistance of dentin bonds prepared with two vs three step adhesives: Effect of EDC. Dent Mater. 2017 (in review).

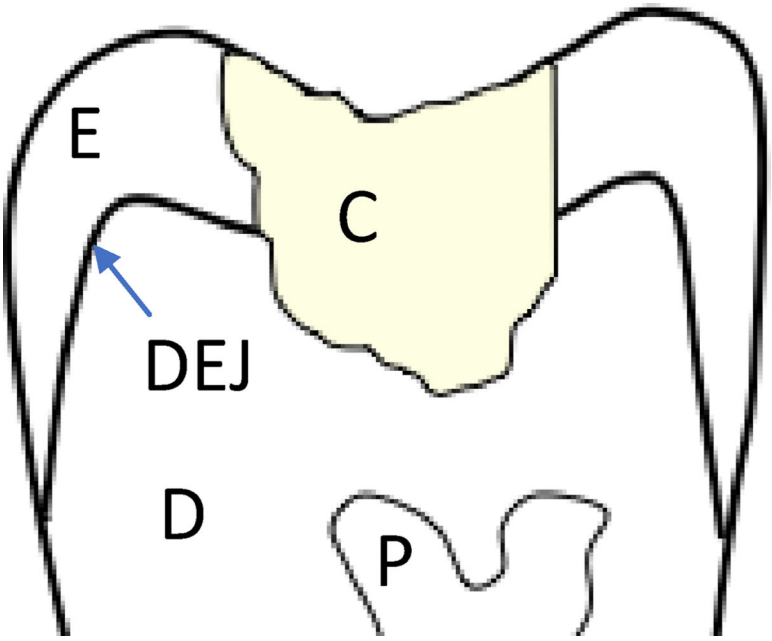

Figure 1.

Schematic diagram for the crown portion of a restored tooth. Highlighted in this diagram are the resin composite restoration (C), the enamel (E), the dentin (D), the pulp (P) and the Dentin Enamel Junction (DEJ). The interface between the composite and surrounding tooth structure is the bonded interface.

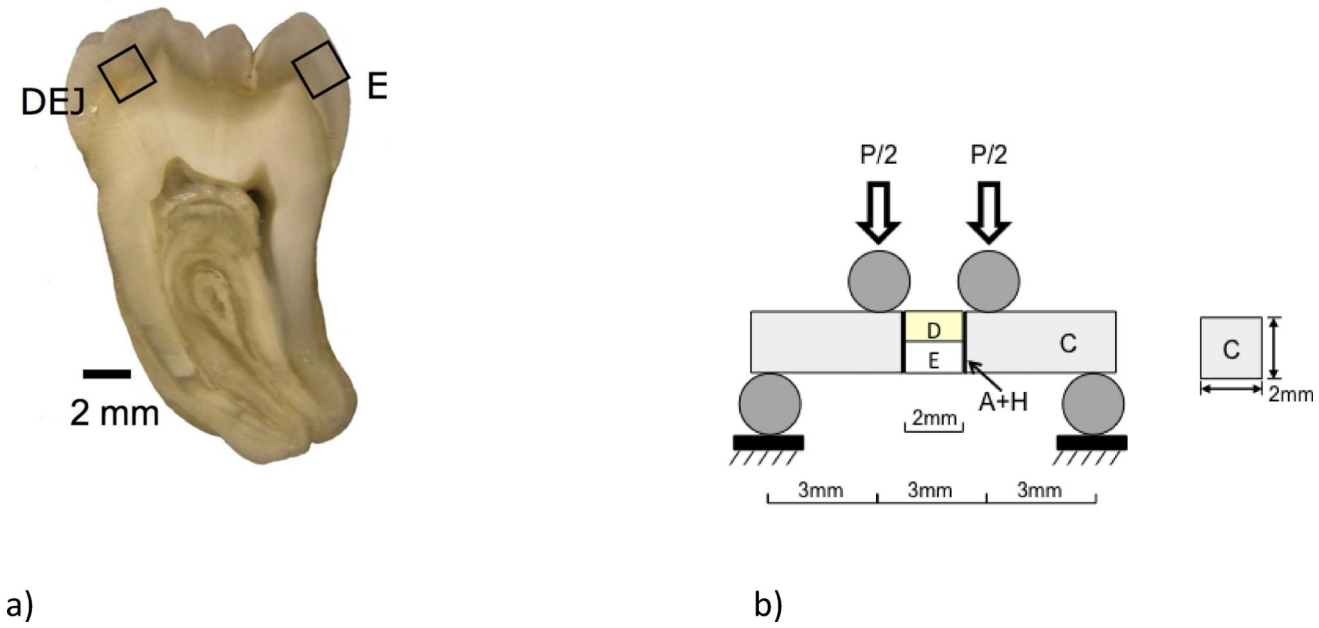

Figure 2.

Preparation of the twin bonded interface specimens and flexural loading. a) A primary tooth section from the bucco-lingual plane with 2 mm thickness. Secondary sectioning was used to prepare 2×2×2 mm^3 cubes of material consisting of enamel only (E), or the Dentin Enamel Junction (DEJ). The specimen geometry after preparation was approximately 2×2×12 mm^3. (b) the four-point flexure configuration for evaluating the bonded interface. For the enamel specimens loading was conducted with either the outer enamel (nearest the occlusal surface) subjected to tension or the inner enamel (nearest the DEJ) subjected to tension. These two configurations are regarded as the “occlusal” and “decussated” arrangements, respectively. The DEJ specimens were arranged for cyclic loading such that the enamel was subjected to cyclic tension.

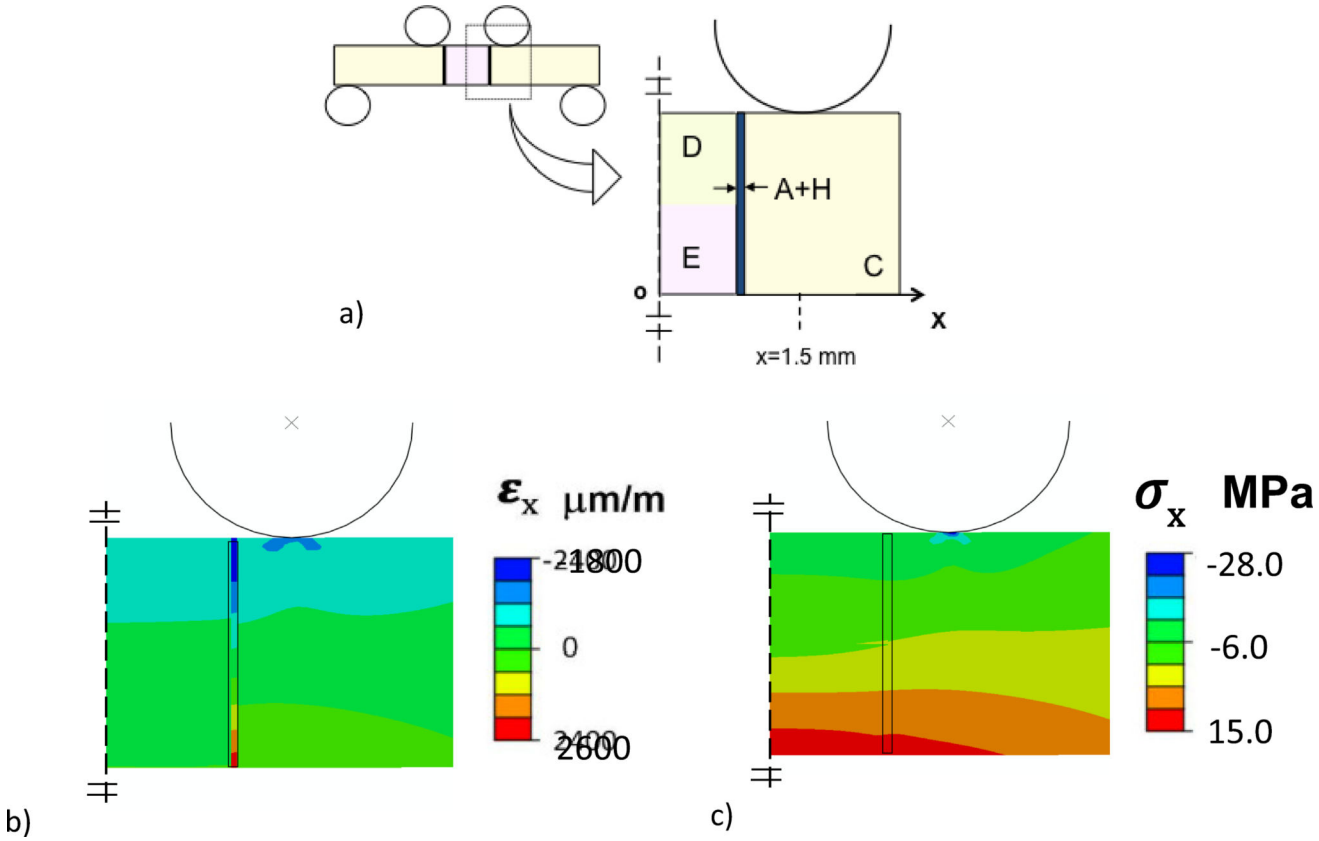

Figure 3.

Details of the Finite Element Analysis (FEA) for four-point loading of the bonded interface specimens with DEJ. The resin composite (C), enamel (E) and the twin bonded interfaces are highlighted, along with the resin adhesive and enamel hybrid layer (A+H). a) Model configuration. b) Normal strain distribution within the beam in the x direction. Red = tensile strain and Blue = compressive strain. c) Normal stress distribution of the beam in the x-direction. The strain and stress distributions in this figure resulted from 10 N load flexure load. Red = tensile stress and Blue = compressive stress.

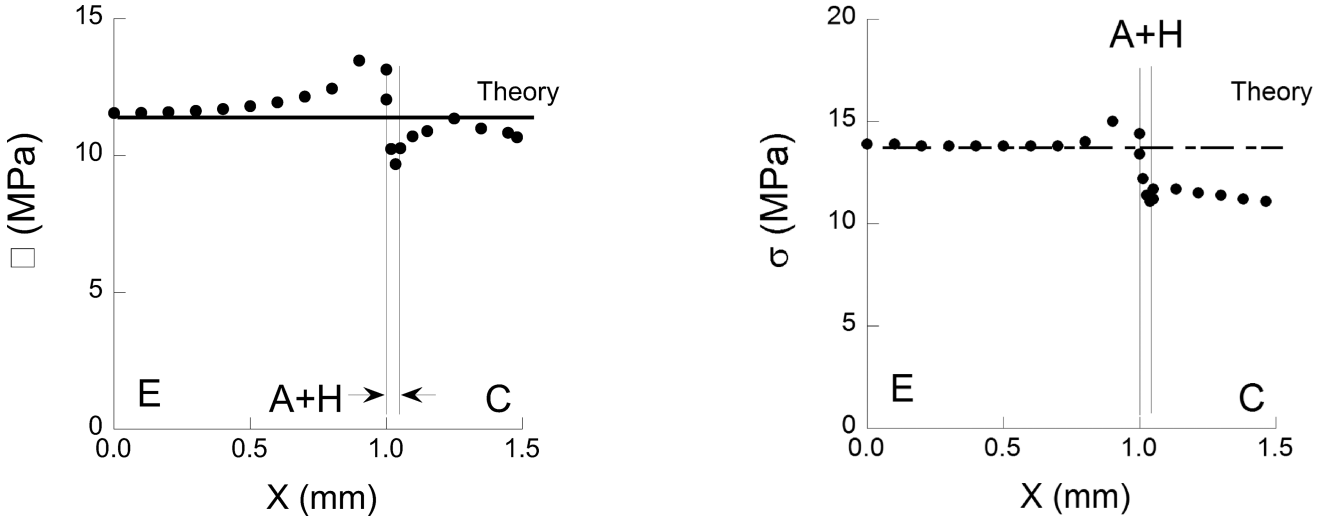

Figure 4.

The normal stress distribution in the x-direction along the tensile surface (i.e. the region of maximum normal stress) of the twin interface specimen for a flexural load of 10 N. The normal stress is acting in the x-direction, normal to the bonded interface. The stress is plotted from the center of the enamel or DEJ section (x=0) to the right, across the adhesive layer and within the resin composite. The stress distribution obtained from the finite element analysis (dotted line) is presented along with that estimated using beam theory (solid line). a) enamel bonding without the DEJ, b) bond including enamel and dentin as shown in Fig 3(a). Note the difference in the axis range for these two plots. In both cases, there is a concentration of stress in the hard tissue adjacent that develops adjacent to the bonded adhesive. The largest stress develops in the bonded interface involving the DEJ.

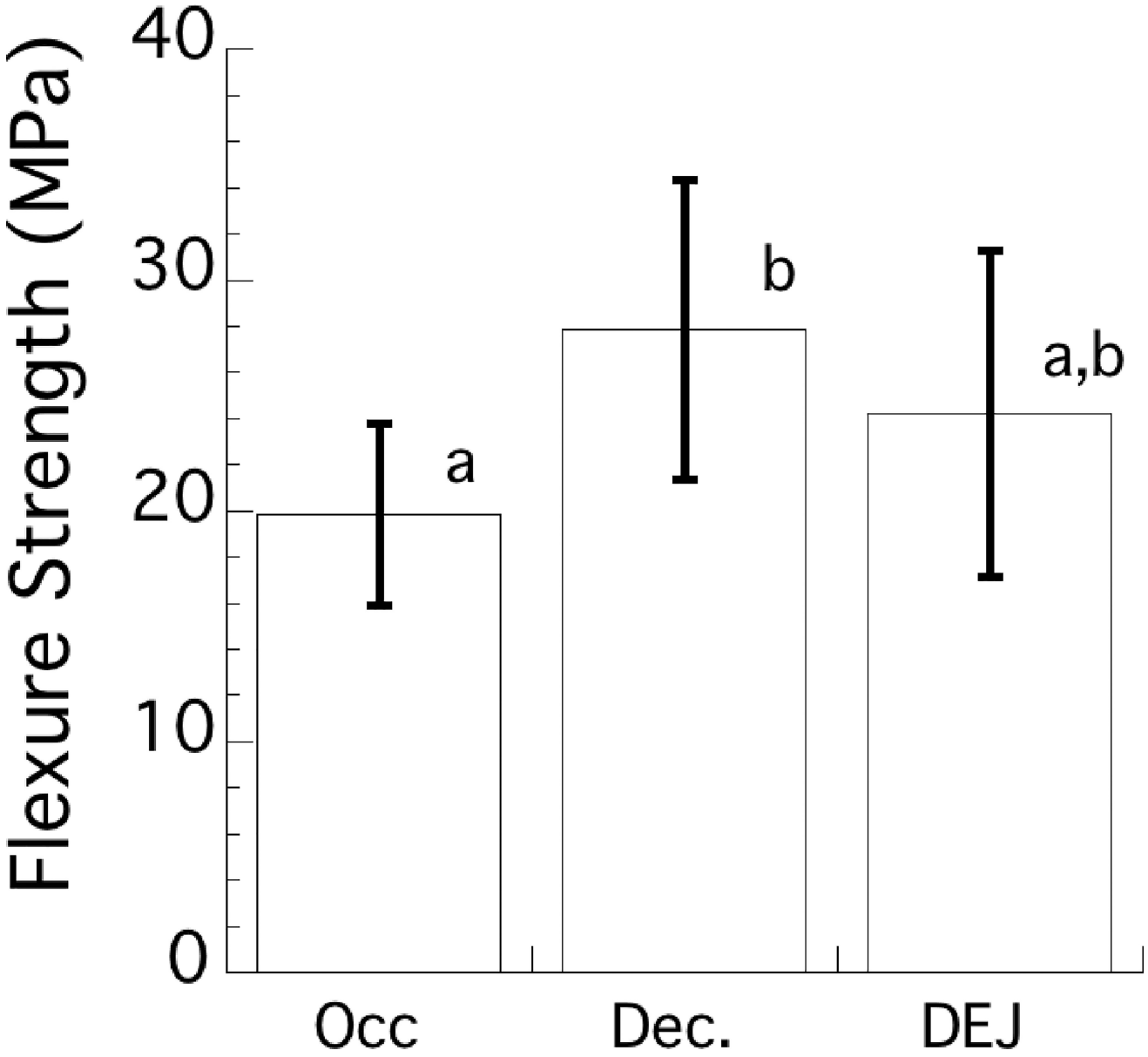

Figure 5.

Flexure strength distribution in terms of the average and standard deviation for adhesive bonds to the enamel and the DEJ. The enamel bonds were oriented such that cyclic tension occurred either on the outer (occlusal) or the inner (decussated) enamel. In the DEJ bonds, cyclic tension always occurred on the enamel side of the bonded interfaces. Columns with the same letter indicate no significant difference.

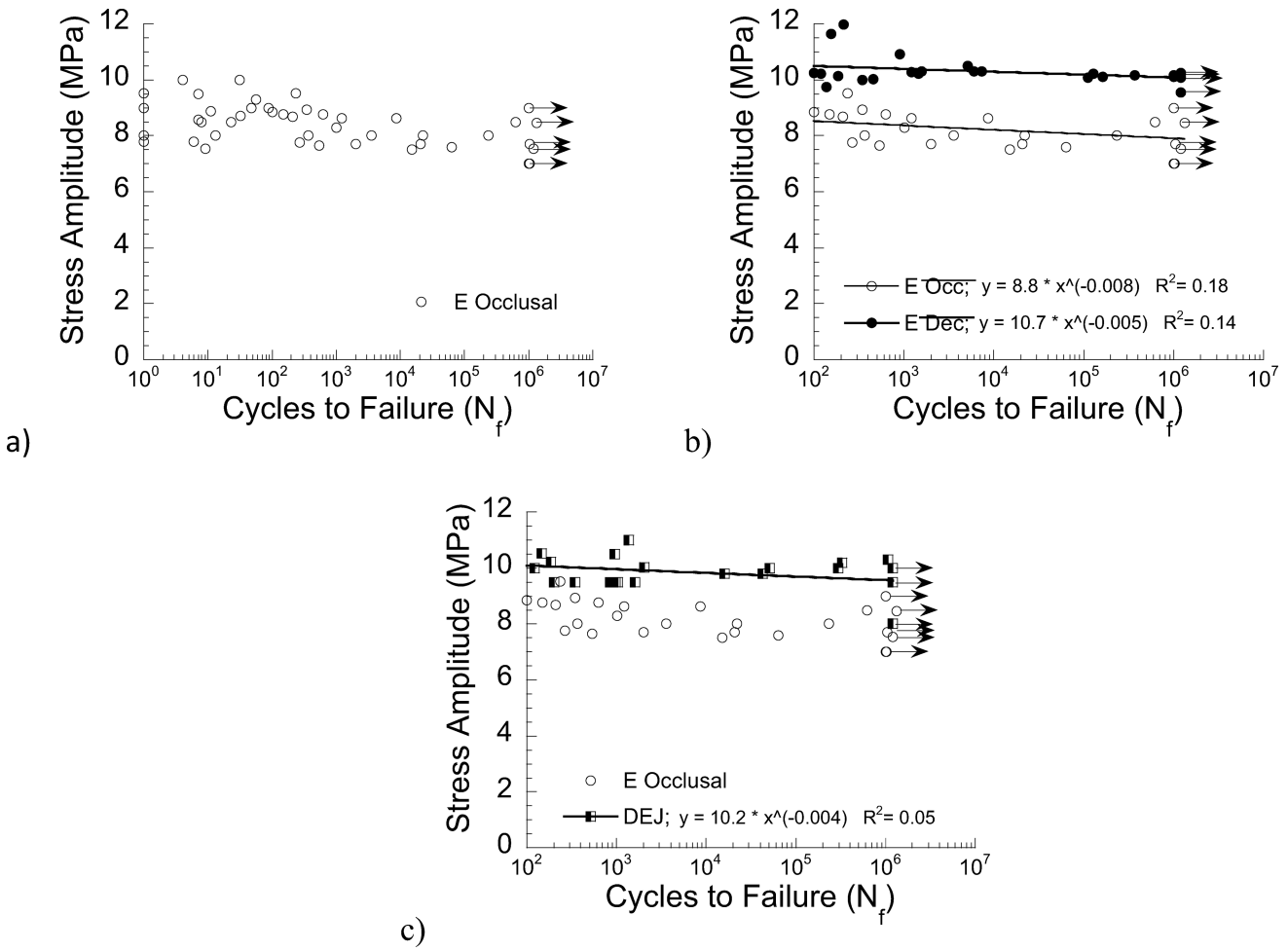

Figure 6.

Fatigue strength distributions resulting from the cyclic loading experiments. a) fatigue life diagram for enamel with occlusal orientation (outer enamel in cyclic tension), b) comparison of fatigue life diagrams for the enamel bonded interface specimens with occlusal and decussated directions. The power law constants (A, B) are also provided for each material system, which describe the fatigue life distributions according to Eqn. 1. c) comparison of fatigue life diagrams for the DEJ with the occlusal enamel. Note that (b) and (c) present the results for specimens with lives of N≥ 100 cycles. All data points represent the result for a single fatigue test and the data points with arrows represent a specimen that did not fail within 1.2×10̂6 cycles, and the test was discontinued.

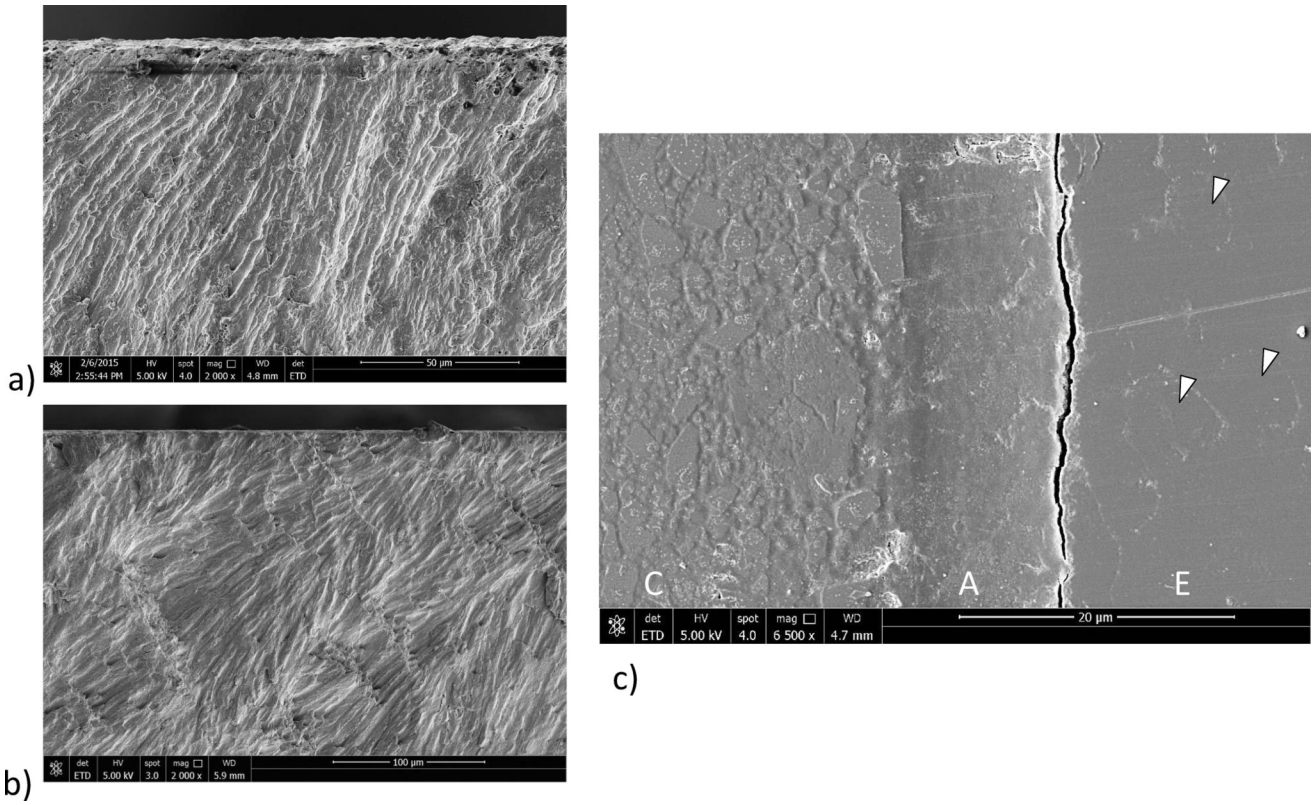

Figure 7.

Images from the enamel bonded interface specimens after fatigue failure. The figures are obtained from the tensile side of the specimens. a) occlusal orientation. Fatigue failure initiated in the enamel. b) decussated orientation. Fatigue failure initiated in the enamel. c) Tensile exterior surface of a decussated enamel specimen that failed due to cyclic loading. Shown here is the twin interface that did not undergo complete failure, but was subjected to cyclic loading. Note the crack in the enamel (E) that is adjacent to the resin adhesive (A). Arrows point to the outline of the individual enamel rods that appear on the tensile surface. C is the resin composite.

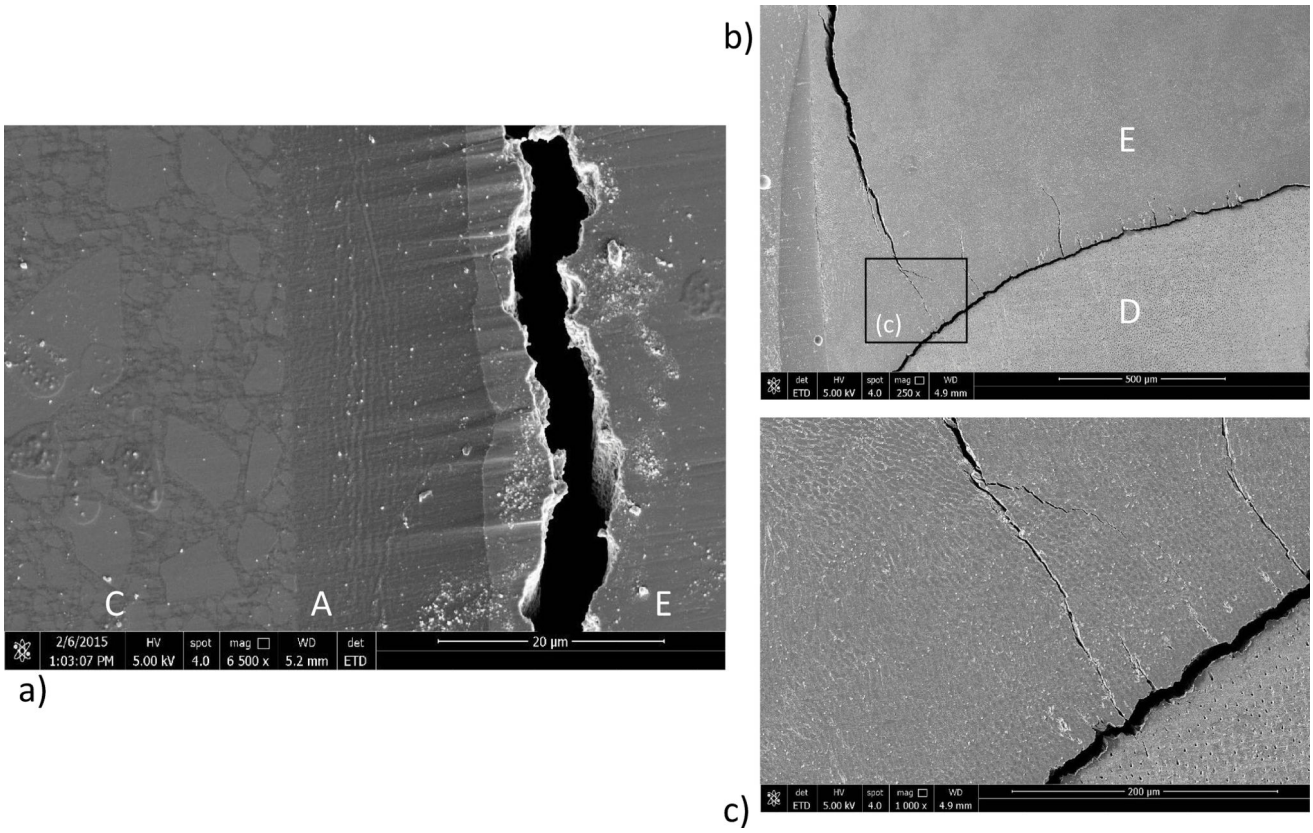

Figure 8.

Images from the DEJ bonded interface specimens after fatigue failure. The figures are obtained from the tensile side of the specimens. a) Tensile exterior surface of the twin interface. Evident are the enamel (E), resin adhesive (A) and resin composite (C). Note the large crack opening displacement. b) crack extending within the enamel towards the DEJ in a specimen that underwent fatigue failure. Shown is the twin interface that did not fail but exhibits the evidence of cyclic loading related damage. c) a more highly magnified view of the image in (b). Note the cracks evident that extend from the DEJ into the enamel along the enamel tufts.